The Journal of Molecular Diagnostics, Vol. 16, No. 2, March 2014

the Journal of Molecular Diagnostics
jmd.amjpathol.org

# A Single-Tube Multiplexed Assay for Detecting *ALK*, *ROS1*, and *RET* Fusions in Lung Cancer

Maruja E. Lira,* Yoon-La Choi,† Sun Min Lim,‡ Shibing Deng,* Donghui Huang,* Mark Ozeck,* Joungho Han,§ Ji Yun Jeong,¶ Hyo Sup Shim,¶ Byoung Chul Cho,‡ Jhingook Kim,‖ Myung-Ju Ahn,§ and Mao Mao*

*From the Oncology Research Unit,* Pfizer Inc, San Diego, California; the Departments of Pathology,† Medical Oncology,§ and Thoracic Surgery,‖ Samsung Medical Center, Sungkyunkwan University School of Medicine, Seoul, Republic of Korea; the Department of Internal Medicine,‡ Yonsei Cancer Center, Yonsei University College of Medicine, Seoul, Republic of Korea; and the Department of Pathology,¶ Kyungpook National University Hospital, Daegu, Republic of Korea*

Accepted for publication November 6, 2013.

Address correspondence to Jhingook Kim, M.D., or Myung-Ju Ahn, M.D., Samsung Medical Center, 81 Ilwon-ro, Gangnam-Gu, Seoul, Republic of Korea; or Mao Mao, M.D., Ph.D., Oncology Research Unit, Pfizer Inc, 10724 Science Center Dr., San Diego, CA 92121. E-mail: jkimsmc@skku.edu, silkahn@skku.edu or mao_m@yahoo.com.

Approximately 7% of non–small cell lung carcinomas (NSCLCs) harbor oncogenic fusions involving *ALK*, *ROS1*, and *RET*. Although tumors harboring *ALK* fusions are highly sensitive to crizotinib, emerging preclinical and clinical data demonstrate that patients with *ROS1* or *RET* fusions may also benefit from inhibitors targeting these kinases. Using a transcript-based method, we designed a combination of 3′ overexpression and fusion-specific detection strategies to detect ALK, ROS1 and RET fusion transcripts in NSCLC tumors. We validated the assay in 295 NSCLC specimens and showed that the assay is highly sensitive and specific. *ALK* results were 100% concordant with fluorescence *in situ* hybridization (FISH) ($n = 52$) and 97.8% concordant with IHC ($n = 179$) [sensitivity, 96.8% (95% CI 91.0%–98.9%); specificity, 98.8% (95% CI 93.6%–99.8%)]. For *ROS1* and *RET*, we also observed 100% concordance with FISH ($n = 46$ and $n = 15$, respectively). We identified seven *ROS1* and 14 *RET* fusion–positive tumors and confirmed the fusion status by RT-PCR and FISH. One *RET* fusion involved a novel partner, cutlike homeobox 1 gene (*CUX1*), yielding an in-frame CUX1-RET fusion. *ROS1* and *RET* fusions were significantly enriched in tumors without *KRAS/EGFR/ALK* alterations. *ALK/ROS1/RET/EGFR/KRAS* alterations were mutually exclusive. As a single-tube assay, this test shows promise as a more practical and cost-effective screening modality for detecting rare but targetable fusions in NSCLC. *(J Mol Diagn 2014, 16: 229–243; http://dx.doi.org/10.1016/j.jmoldx.2013.11.007)*

Lung cancer is the leading cause of cancer-related mortality worldwide, with non–small cell lung carcinoma (NSCLC) accounting for 85% of all lung cancer cases. Recent advances in the identification of a subset of patients with specific genomic alterations and the successful clinical translation of targeted therapies provide a strong rationale for the development of robust screening modalities to identify such patients.

Fusions with *ALK* (anaplastic lymphoma kinase) occur in approximately 5% of NSCLC cases. The DNA rearrangement leads to expression of a constitutively active kinase protein. Tumors harboring *ALK* rearrangement rely specifically on the chimeric oncoprotein for progression and are sensitive to ALK inhibitors, such as crizotinib, a US Food and Drug Administration–approved drug for the treatment of *ALK* fusion–positive NSCLC.[1] *ROS1* (c-ros oncogene 1) is a receptor tyrosine kinase. *ROS1* fusions may play a role in the tumorigenesis of glioblastoma and cholangiocarcinoma and have been found in 1% to 2% of NSCLCs. There are 12 *ROS1* fusions with seven different partners identified in NSCLC.[2–8] A recent clinical study demonstrated that patients with NSCLC with *ROS1* fusions may benefit from crizotinib treatment.[9] *RET* (rearranged during transfection) is also a receptor tyrosine kinase that has been shown mutated (point mutations and fusions) in thyroid cancer. Several

Supported in part by grant A092255 from the Korean Health Technology R&D Project, Ministry of Health & Welfare, Republic of Korea.

M.E.L., Y.-L.C., and S.M.L. contributed equally to this work.

Disclosures: M.E.L., S.D., D.H., M.O., and M.M. are employees of and own stock in Pfizer Inc. Mirax (Republic of Korea) supported the ZytoVision *ROS1* FISH and *RET* FISH tests.


http://dx.doi.org/10.1016/j.jmoldx.2013.11.007

recent cancer genome sequencing studies identified *RET* fusions in 1% to 2% of NSCLC,[10,11] most frequently involving *KIF5B* and *CCDC6* as fusion partners. Recent preclinical data have shown that clinically available tyrosine kinase inhibitors with anti-RET activity, such as sunitinib, sorafenib, and vandetanib, may offer potential treatments for *RET* fusion–positive tumors.[5] Indeed, early clinical data from three RET fusion–positive patients treated with cabozantinib, a RET inhibitor, showed quite promising results.[12]

Current methods for detecting *ALK*, *ROS1,* and *RET* fusions include fluorescence *in situ* hybridization (FISH), immunohistochemical (IHC) analysis, and RT-PCR, with each test offering its own advantages and disadvantages. FISH, the current US Food and Drug Administration–approved companion diagnostic test for detecting *ALK* fusions for crizotinib treatment, is complex and has limitations in terms of cost and throughput, making it impractical for screening large numbers of patients for the detection of rare but potentially clinically relevant oncogenic fusions. To explore a single-tube and more practical screening modality, we developed and evaluated the performance of a transcript-based assay to simultaneously detect the presence of *ALK*, *ROS1,* and *RET* fusions in NSCLC clinical specimens.

## Materials and Methods

### Patient Samples, Mutations, and IHC and FISH Analyses

NSCLC specimens were obtained from Samsung Medical Center (SMC) and Yonsei Cancer Center (YCC) (Seoul, Republic of Korea) with previous full informed consent from the patient and with approvals from SMC and YCC ethical committees/internal review boards. A total of 295 surgically resected lung adenocarcinoma samples were analyzed as four cohorts. Set 1 ($n = 94$) was enriched for *ALK* fusion–positive patients as detected by IHC and wild type for *KRAS* and *EGFR*. Set 2 ($n = 85$) was negative for *ALK* fusion (also by IHC) and also wild type for *EGFR* and *KRAS*. FISH data for *ALK* were available for 52 individuals in sets 1 and 2. Set 3 ($n = 84$) consisted of never-smokers with lung adenocarcinoma unselected for *ALK*, *EGFR,* and *KRAS* mutation status. Set 4 patients ($n = 32$) were never-smokers with lung adenocarcinoma previously characterized for *ROS1* fusion by FISH.[13] Sets 1 to 3 were obtained from SMC and set 4 from YCC. All the patients were Korean in ethnicity. *ALK* FISH and IHC tests for sets 1 and 2 and *ROS1* FISH tests for set 4 have been described in previous publications.[13,14] *ROS1* FISH and *RET* FISH tests for the tumors selected from sets 2 and 3 were performed using ZytoLight SPEC ROS1 and RET dual-color break-apart probes (ZytoVision GmbH, Bremerhaven, Germany) according to the manufacturer's instructions. *EGFR* and *KRAS* mutation status was determined as follows: sets 1 and 2, Sanger sequencing; set 3, the MassARRAY system (Sequenom Inc., San Diego, CA); and set 4, PNAClamp mutation detection kits (Panagene Inc., Daejeon, Republic of Korea). Control lung cancer cell line HCC78 (*ROS*1 positive)[6] was obtained from Deutsche Sammlung von Mikroorganismen und Zellkulturen GmbH (Braunschweig Germany); control lung cancer cell lines NCI-H3122 (*ALK* positive) and A549 (*ALK, ROS1,* and *RET* wild type)[14–16] were obtained from ATCC (Manassas, VA).

### *ALK*, *ROS1,* and *RET* Fusion Assay

The probe sets were custom designed and synthesized by NanoString Technologies (Seattle, WA). Hybridization, sample cleanup, and digital reporter counts were performed according to the manufacturer's protocol. RNA samples from sets 1, 2, and 4 were prepared from two to three formalin-fixed, paraffin-embedded (FFPE) tissue slide sections (10 μm thick) as described previously.[14] RNA samples from set 3 were obtained from fresh frozen tissues using the RNeasy mini kit (Qiagen Inc., Valencia, CA). Concentration was assessed by spectrophotometry using the NanoDrop 8000 (Thermo Scientific, Wilmington, DE).

Total RNA was hybridized to a multiplexed mixture of custom-designed capture and reporter probes complementary to *ALK*, *ROS1,* and *RET* target sequences (Table 1). For FFPE-derived (degraded) and fresh frozen (intact) RNA, 500 and 250 ng of RNA were used, respectively. Hybridization, cleanup, imaging, and counting were processed according to a previous publication.[14]

### Data Analysis and Threshold Determination

Data were normalized in two steps as described in a previous publication.[14] Technical background was determined from the eight ERCC-negative control probes. Means and SDs were calculated from the negative controls, and a background threshold (*B*) was defined as the mean plus 2 SD. A target with a normalized intensity value above this threshold was scored as "present." A biological background ($B_5$) was defined as follows for 5′ probes of individual genes based on the median of all 5′ probe intensity for that gene across all samples and their SD:

$$B_5 = median + 2 \times SMAD \quad (1)$$

where $S_{MAD} = 1.4826$*MAD is the SD calculated from the median absolute deviation (MAD) from median for normally distributed data. It is a more robust measure of variability than the sample SD. Normalized intensity from sample replicates was averaged to obtain an averaged patient intensity for each probe and patient.

To summarize the 3′ overexpression, we defined a 3′ overexpression score (ie, the ALK 3′/5′ ratio) for each patient and gene as follows:

$$R35 = 3'/5' = \frac{E_3}{\max(A_5, B_t)} \quad (2)$$

**Table 1** ALK, ROS1, and RET NanoString Target Sequences

| Assay type | Reporter | Probe location | Accession No.* | Target sequence |
|---|---|---|---|---|
| 3′/5′ | ALK 5′-1 | ALK exon 1 | NG_009445.1 | 5′-GCGCAGCGCGGGGGCTGGGATTCACGCCCAGAAG TTCAGCAGGCAGACAGTCCGAAGCCTTCCCGCAGC GGAGAGATAGCTTGAGGGTGCGCAAGACGGC-3′ |
| 3′/5′ | ALK 5′-2 | ALK exon 1 | NG_009445.1 | 5′-CTACTCGCGCCTGCAGAGGAAGAGTCTGGCAGTT GACTTCGTGGTGCCCTCGCTCTTCCGTGTCTACGC CCGGGACCTACTGCTGCCACCATCCTCCTCG-3′ |
| 3′/5′ | ALK 5′-3 | ALK exon 5 | NG_009445.1 | 5′-ACAGTGCTCCAGGGAAGAATCGGGCGTCCAGACA ACCCATTTCGAGTGGCCCTGGAATACATCTCCAGT GGAAACCGCAGCTTGTCTGCAGTGGACTTCT-3′ |
| 3′/5′ | ALK 5′-4 | ALK exon 18 | NG_009445.1 | 5′-TAAAAGTGATGGAAGGCCACGGGGAAGTGAATAT TAAGCATTATCTAAACTGCAGTCACTGTGAGGTAG ACGAATGTCACATGGACCCTGAAAGCCACAA-3′ |
| 3′/5′ | ALK 3′-1 | ALK exon 22/23 | NG_009445.1 | 5′-AGACGCTGCCTGAAGTGTGCTCTGAACAGGACGA ACTGGATTTCCTCATGGAAGCCCTGATCATCAGCA AATTCAACCACCAGAACATTGTTCGCTGCAT-3′ |
| 3′/5′ | ALK 3′-2 | ALK exon 26/27 | NG_009445.1 | 5′-CAGAGGCCTTCATGGAAGGAATATTCACTTCTAA AACAGACACATGGTCCTTTGGAGTGCTGCTATGGG AAATCTTTTCTCTTGGATATATGCCATACCC-3′ |
| 3′/5′ | ALK 3′-3 | ALK exon 29 | NG_009445.1 | 5′-TTGTGGAACCCAACGTACGGCTCCTGGTTTACAG AGAAACCCACCAAAAAGAATAATCCTATAGCAAAG AAGGAGCCACACGACAGGGGTAACCTGGGGC-3′ |
| 3′/5′ | ALK 3′-4 | Exon 29 (3′ UTR) | NG_009445.1 | 5′-GTCGCACACTCACTTCTCTTCCTTGGGATCCCTA AGACCGTGGAGGAGAGAGAGGCAATGGCTCCTTCA CAAACCAGAGACCAAATGTCACGTTTTGTTT-3′ |
| 3′/5′ | ROS1 5′-1 | ROS1 exon 1 (5′ UTR) | NM_002944.2 | 5′-ACAAACAAAGCAAAATCCATCAGCTACTCCTCCA ATTGAAGTGATGAAGCCCAAATAATTCATATAGCA AAATGGAGAAAATTAGACCGGCCATCTAAAA-3′ |
| 3′/5′ | ROS1 5′-2 | ROS1 exon 18/19 | NM_002944.2 | 5′-TCAAGAAATAGGTCAGAAAACCAGTGTCTCTGTT TTGGAACCAGCCAGATTTAATCAGTTCACAATTAT TCAGACATCCCTTAAGCCCCTGCCAGGGAAC-3′ |
| 3′/5′ | ROS1 5′-3 | ROS1 exon 24 | NM_002944.2 | 5′-GCACCTCTACTTTGCACTGAAAGAATCACAAAAT GGAATGCAAGTATTTGATGTTGATCTTGAACACAA GGTGAAATATCCCAGAGAGGTGAAGATTCAC-3′ |
| 3′/5′ | ROS1 5′-4 | ROS1 exon 29/30 | NM_002944.2 | 5′-CTCTAAGACAAAGTGAATTTCCAAATGGAAGGCT CACTCTCCTTGTTACTAGACTGTCTGGTGGAAATA TTTATGTGTTAAAGGTTCTTGCCTGCCACTC-3′ |
| 3′/5′ | ROS1 3′-1 | ROS1 exon37 | NM_002944.2 | 5′-GGAGAAGATTGAATTCCTGAAGGAGGCACATCTG ATGAGCAAATTTAATCATCCCAACATTCTGAAGCA GCTTGGAGTTTGTCTGCTGAATGAACCCCAA-3′ |
| 3′/5′ | ROS1 3′-2 | ROS1 exon 40 | NM_002944.2 | 5′-ACCTTGTAGACCTGTGTGTAGATATTTCAAAAGG CTGTGTCTACTTGGAACGGATGCATTTCATTCACA GGGATCTGGCAGCTAGAAATTGCCTTGTTTC-3′ |
| 3′/5′ | ROS1 3′-3 | ROS1 exon 41/42 | NM_002944.2 | 5′-GAAATTGTCCTGATGATCTGTGGAATTTAATGAC CCAGTGCTGGGCTCAAGAACCCGACCAAAGACCTA CTTTTCATAGAATTCAGGACCAACTTCAGTT-3′ |
| 3′/5′ | ROS1 3′-4 | ROS1 exon 43 (3′ UTR) | NM_002944.2 | 5′-AGAGAGTTGAGATAAACACTCTCATTCAGTAGTT ACTGAAAGAAAACTCTGCTAGAATGATAAATGTCA TGGTGGTCTATAACTCCAAATAAACAATGCA-3′ |
| 3′/5′ | RET 5′-1 | RET exon 1-2 | NM_020630.4 | 5′-GCTGCTGCTGCCGCTGCTAGGCAAAGTGGCATTG GGCCTCTACTTCTCGAGGGATGCTTACTGGGAGAA GCTGTATGTGGACCAGGCGGCCGGCACGCCC-3′ |
| 3′/5′ | RET 5′-2 | RET exon 2-3 | NM_020630.4 | 5′-TCAGTGTCCGCAACCGCGGCTTTCCCCTGCTCAC CGTCTACCTCAAGGTCTTCCTGTCACCCACATCCC TTCGTGAGGGCGAGTGCCAGTGGCCAGGCTG-3′ |
| 3′/5′ | RET 5′-3 | RET exon 6-7 | NM_020630.4 | 5′-CGTGAGCAGGAGGGCTCGCCGATTTGCCCAGATC GGGAAAGTCTGTGTGGAAAACTGCCAGGCATTCAG TGGCATCAACGTCCAGTACAAGCTGCATTCC-3′ |
| 3′/5′ | RET 5′-4 | RET exon 11 | NM_020630.4 | 5′-TGCGACGAGCTGTGCCGCACGGTGATCGCAGCCG CTGTCCTCTTCTCCTTCATCGTCTCGGTGCTGCTG TCTGCCTTCTGCATCCACTGCTACCACAAGT-3′ |

(*table continues*)

**Table 1** (*continued*)

| Assay type | Reporter | Probe location | Accession No.* | Target sequence |
|---|---|---|---|---|
| 3′/5′ | RET 3′-1 | RET exon 14-15 | NM_020630.4 | 5′-AGGGGATGCAGTATCTGGCCGAGATGAAGCTCGT TCATCGGGACTTGGCAGCCAGAAACATCCTGGTAG CTGAGGGGCGGAAGATGAAGATTTCGGATTT-3′ |
| 3′/5′ | RET 3′-2 | RET exon 15-16-17 | NM_020630.4 | 5′-AGGAGCCAGGGTCGGATTCCAGTTAAATGGATGG CAATTGAATCCCTTTTTGATCATATCTACACCACG CAAAGTGATGTATGGTCTTTTGGTGTCCTGC-3′ |
| 3′/5′ | RET 3′-3 | RET exon 18 | NM_020630.4 | 5′-AAGACCTGGAGAAGATGATGGTTAAGAGGAGAGA CTACTTGGACCTTGCGGCGTCCACTCCATCTGACT CCCTGATTTATGACGACGGCCTCTCAGAGGA-3′ |
| 3′/5′ | RET 3′-4 | RET exon 19 UTR | NM_020630.4 | 5′-TTTCCCTTACCCACCTTCAGGACGGTTGTCACTT ATGAAGTCAGTGCTAAAGCTGGAGCAGTTGCTTTT TGAAAGAACATGGTCTGTGGTGCTGTGGTCT-3′ |
| Fusion | Fusion_ALKe20 | EML4-ALK_E13:A20 | PFUS_001.1 | 5′-ATATGGAGCAAAACTACTGTAGAGCCCACACCTG GGAAAGGACCTAAAGTGTACCGCCGGAAGCACCAG GAGCTGCAAGCCATGCAGATGGAGCTGCAG-3′ |
| Fusion | Fusion_ALKe20 | EML4-ALK_E20:A20 | PFUS_002.1 | 5′-GACAACAAGTATATAATGTCTAACTCGGGAGACT ATGAAATATTGTACTTGTACCGCCGGAAGCACCAG GAGCTGCAAGCCATGCAGATGGAGCTGCAG-3′ |
| Fusion | Fusion_ALKe20 | EML4-ALK_E6:A20 | PFUS_003.1 | 5′-AAAGTTACCAAAACTGCAGACAAGCATAAAGATG TCATCATCAACCAAGTGTACCGCCGGAAGCACCAG GAGCTGCAAGCCATGCAGATGGAGCTGCAG-3′ |
| Fusion | Fusion_ALKe20 | EML4-ALK_E2:A20 | PFUS_006.1 | 5′-ATCTCTGAAGATCATGTGGCCTCAGTGAAAAAAT CAGTCTCAAGTAAAGTGTACCGCCGGAAGCACCAG GAGCTGCAAGCCATGCAGATGGAGCTGCAG-3′ |
| Fusion | Fusion_ALKe20 | EML4-ALK_E18:A20 | PFUS_008.1 | 5′-ATCCACACAGACGGGAATGAACAGCTCTCTGTGA TGCGCTACTCAATAGTGTACCGCCGGAAGCACCAG GAGCTGCAAGCCATGCAGATGGAGCTGCAG-3′ |
| Fusion | Fusion_ALKe20 | KIF5B-ALK_K24:A20 | PFUS_013.1 | 5′-GCAGTCAGGTCAAAGAATATGGCCAGAAGAGGGC ATTCTGCACAGATTGTGTACCGCCGGAAGCACCAG GAGCTGCAAGCCATGCAGATGGAGCTGCAG-3′ |
| Fusion | Fusion_ALKe20 | TFG-ALK_T5:A20 | PFUS_016.1 | 5′-CAGCAGCCACCATATACAGGAGCTCAGACTCAAG CAGGTCAGATTGAAGTGTACCGCCGGAAGCACCAG GAGCTGCAAGCCATGCAGATGGAGCTGCAG-3′ |
| Fusion | Fusion_ALKe20 | KIF5B-ALK_K17:A20 | PFUS_031.1 | 5′-TTGGAGGAATCTGTCGATGCCCTCAGTGAAGAAC TAGTCCAGCTTCGAGCACAAGTGTACCGCCGGAAG CACCAGGAGCTGCAAGCCATGCAGATGGAGC-3′ |
| Fusion | Fusion_ROS1e32 | SLC34A2-ROS1_S4:R32 | PFUS_020.1 | 5′-GTGTGCTCCCTGGATATTCTTAGTAGCGCCTTCC AGCTGGTTGGAGCTGGAGTCCCAAATAAACCAGGC ATTCCCAAATTACTAGAAGGGAGTAA-3′ |
| Fusion | Fusion_ROS1e32 | CD74-ROS_C6:R32 | PFUS_030.1 | 5′-AATGAGCAGGCACTCCTTGGAGCAAAAGCCCACT GACGCTCCACCGAAAGCTGGAGTCCCAAATAAACC AGGCATTCCCAAATTACTAGAAGGGAGTAAA-3′ |
| Fusion | Fusion_ROS1e32 | SDC4-ROS1_S2:R32 | PFUS_024.1 | 5′-GCCCGGGCAGGAATCTGATGACTTTGAGCTGTCT GGCTCTGGAGATCTGGCTGGAGTCCCAAATAAACC AGGCATTCCCAAATTACTAGAAGGGAGTAAA-3′ |
| Fusion | Fusion_ROS1e32 | SLC34A2-ROS1_S13 del2046:R32 | PFUS_034.1 | 5′-CAAGGCTCCTGAGACCTTTGATAACATAACCATT AGCAGAGAGGCTCAGGCTGGAGTCCCAAATAAACC AGGCATTCCCAAATTACTAGAAGGGAGTAAA-3′ |
| Fusion | SLC34A2-ROS1 V2 | SLC34A2-ROS1_S4:R34 | PFUS_021.1 | 5′-TTTTCGTGTGCTCCCTGGATATTCTTAGTAGCGC CTTCCAGCTGGTTGGAGATGATTTTTGGATACCAG AAACAAGTTTCATACTTACTATTATAGTTGG-3′ |
| Fusion | EZR-ROS1 | EZR-ROS1_E10:R34 | PFUS_032.1 | 5′-AAGGAGGAGTTGATGCTGCGGCTGCAGGACTATG AGGAGAAGACAAAGAAGGCAGAGAGAGATGATTTT TGGATACCAGAAACAAGTTTCATACTTACTA-3′ |
| Fusion | SDC4-ROS1 | SDC4-ROS1_S4:R34 | PFUS_033.1 | 5′-GGTGTCAATGTCCAGCACTGTGCAGGGCAGCAAC ATCTTTGAGAGAACGGAGGTCCTGGCAGATGATTT TTGGATACCAGAAACAAGTTTCATACTTACT-3′ |
| Fusion | FIG-ROS1 V1 | GOPC-ROS1_G8:R35 | PFUS_023.1 | 5′-CCCTGGTGCTAGTTGCAAAGACACAAGTGGGGAA ATCAAAGTATTACAAGTCTGGCATAGAAGATTAAA GAATCAAAAAAGTGCCAAGGAAGGGGTGACA-3′ |

(*table continues*)

**Table 1** (*continued*)

| Assay type | Reporter | Probe location | Accession No.* | Target sequence |
|---|---|---|---|---|
| Fusion | TPM3-ROS1 | TPM3-ROS1_T8:R35 | PFUS_035.1 | 5′-AGTTTGCTGAGAGATCGGTAGCCAAGCTGGAAAA GACAATTGATGACCTGGAAGTCTGGCATAGAAGAT TAAAGAATCAAAAAAGTGCCAAGGAAGGGGT-3′ |
| Fusion | LRIG3-ROS1 | LRIG3-ROS1_L16:R35 | PFUS_027.1 | 5′-AGTTTGTCACATCTTCAGGTGCTGGATTTTTCTT ACCACAACATGACAGTAGTGTCTGGCATAGAAGAT TAAAGAATCAAAAAAGTGCCAAGGAAGGGGT-3′ |
| Fusion | FIG-ROS1 V2 | GOPC-ROS1_G4:R36 | PFUS_022.1 | 5′-TATGGGGCGAGACTAGCTGCCAAGTACTTGGATA AGGAACTGGCAGGAAGTACTCTTCCAACCCAAGAG GAGATTGAAAATCTTCCTGCCTTCCCTCGGG-3′ |
| Fusion | Fusion_RETe12 | KIF5B-RET_K15:R12 | PFUS_028.1 | 5′-AAGACCTTGCAGAAATAGGAATTGCTGTGGGAAA TAATGATGTAAAGGAGGATCCAAAGTGGGAATTCC CTCGGAAGAACTTGGTTCTTGGAAAAACTCT-3′ |
| Fusion | Fusion_RETe12 | KIF5B-RET_K16:R12 | PFUS_025.1 | 5′-AAGAAAATGAAAAGGAGTTAGCAGCATGTCAGCT TCGTATCTCTCAAGAGGATCCAAAGTGGGAATTCC CTCGGAAGAACTTGGTTCTTGGAAAAACTCT-3′ |
| Fusion | Fusion_RETe12 | KIF5B-RET_K22:R12 | PFUS_026.1 | 5′-ACCTGCGCAAACTCTTTGTTCAGGACCTGGCTAC AAGAGTTAAAAAGGAGGATCCAAAGTGGGAATTCC CTCGGAAGAACTTGGTTCTTGGAAAAACTCT-3′ |
| Fusion | Fusion_RETe12 | KIF5B-RET_K23:R12 | PFUS_029.1 | 5′-CCTTTCTTGAAAATAATCTTGAACAGCTCACTAA AGTGCACAAACAGGAGGATCCAAAGTGGGAATTCC CTCGGAAGAACTTGGTTCTTGGAAAAACTCT-3′ |
| Fusion | Fusion_RETe12 | CCDC6-RET_C1:R12 | PFUS_039.1 | 5′-GGAGGAGAACCGCGACCTGCGCAAAGCCAGCGTG ACCATCGAGGATCCAAAGTGGGAATTCCCTCGGAA GAACTTGGTTCTTGGAAAAAC-3′ |
| Fusion | KIF5B-RETe8 | KIF5B-RET_K24:R8 | PFUS_036.1 | 5′-CAGTCAGGTCAAAGAATATGGCCAGAAGAGGGCA TTCTGCACAGATTGATGTGGCCGAGGAGGCGGGCT GCCCCCTGTCCTGTGCAGTCAGCAAGAGA-3′ |
| Fusion | Fusion_RETe11 | KIF5B-RET_K15:R11 | PFUS_037.1 | 5′-AGACCTTGCAGAAATAGGAATTGCTGTGGGAAAT AATGATGTAAAGATCCACTGTGCGACGAGCTGTGC CGCACGGTGATCGCAGCCGCTGTCCTC-3′ |
| Fusion | Fusion_RETe11 | KIF5B-RET_K24:R11 | PFUS_038.1 | 5′-GTCAGGTCAAAGAATATGGCCAGAAGAGGGCATT CTGCACAGATTGATCCACTGTGCGACGAGCTGTGC CGCACGGTGATCGCAGCCGCTGTCCTC-3′ |
| Endogenous | GAPDH | GAPDH exon 1-2 | NM_002046.3 | 5′-TCCTCCTGTTCGACAGTCAGCCGCATCTTCTTTT GCGTCGCCAGCCGAGCCACATCGCTCAGACACCAT GGGGAAGGTGAAGGTCGGAGTCAACGGATTT-3′ |
| Endogenous | OAZ1 | OAZ1 exon 2-3 | NM_004152.2 | 5′-GGTGGGCGAGGGAATAGTCAGAGGGATCACAATC TTTCAGCTAACTTATTCTACTCCGATGATCGGCTG AATGTAACAGAGGAACTAACGTCCAACGACA-3′ |
| Endogenous | POLR2A | POLR2A exon 20-21 | NM_000937.2 | 5′-TTCCAAGAAGCCAAAGACTCCTTCGCTTACTGTC TTCCTGTTGGGCCAGTCCGCTCGAGATGCTGAGAG AGCCAAGGATATTCTGTGCCGTCTGGAGCAT-3′ |
| Endogenous | GUSB | GUSB exon 4-5 | NM_000181.1 | 5′-CGGTCGTGATGTGGTCTGTGGCCAACGAGCCTGC GTCCCACCTAGAATCTGCTGGCTACTACTTGAAGA TGGTGATCGCTCACACCAAATCCTTGGACCC-3′ |

*Accessed at http://www.ncbi.nlm.nih.gov/genbank.

GAPDH, glyceraldehydes-3-phosphate dehydrogenase; GUSB, glucuronidase beta; OAZ1, ornithine decarboxylase antizyme 1; POLR2A, polymerase (RNA) II (DNA directed) polypeptide A; UTR, untranslated region.

where $E_3$ is the geometric mean of 3′ probe expression of individual genes (ALK, ROS1, or RET), and $A_5$ is the median of the corresponding 5′ probe expression; $B_t$ is the maximum of the technical and biological background threshold defined previously herein [$B_t = max(B,B_5)$]. The 3′ probes usually have higher intensity and tend to follow a log-normal distribution, whereas the 5′ probes have lower intensity and are more normally distributed. For this reason we used the geometric mean for 3′ probes and the median for 5′ probes. Using background threshold $B_t$ to floor the denominator prevents an extremely small 5′ expression value that could artificially inflate the score.

We defined a fusion probe background in a similar manner. For each fusion probe a background threshold was defined as the median normalized intensity plus 2 SDs or $B$, whichever was larger:

$$FB = max(B, median + 2 \times SMAD) \quad (3)$$

where $S_{MAD} = 1.4826$*MAD.

Fusion prediction for individual samples was made based on both the 3′/5′ ratio (*R35*) and fusion probe expression (*F* ). A fusion is detected if the 3′/5′ ratio is larger than a prespecified threshold or if at least one fusion probe is above a threshold.

Percentage concordance was calculated between two platforms, and its 95% CI was computed using the Wilson score method. The Cohen kappa statistic was also calculated for concordance analysis. Data were analyzed using standard R software version 2.13.1 (*http://www.r-project.org*). Concordance analysis was conducted using SAS software version 9.2 (SAS Institute, Inc., Cary, NC).

### RT-PCR and Sequencing

The precise ALK, ROS1, and RET fusion variants were determined by RT-PCR, followed by Sanger sequencing. The RNA UltraSense one-step RT-PCR kit (Life Technologies, Carlsbad, CA) was used to generate RT-PCR products, modifying the protocol such that the RT-PCR reaction was performed in two steps. First-strand cDNA was initially synthesized using gene-specific primers (Table 2). cDNA was subdivided into different PCR reactions using the appropriate fusion variant primers, and PCR products were separated on a 2% E-Gel SizeSelect agarose gel (Invitrogen, Carlsbad, CA). In reactions producing a PCR product of the expected size, the amplicons were gel purified and sequenced using a 3700 ABI Prism sequencer (Applied Biosystems, Foster City, CA).

*CUX1-RET* fusion was discovered using the anchored multiplex PCR assay (ArcherDx Inc., Boulder, CO). The assay uses total nucleic acids extracted from the FFPE specimen without genomic DNA and ribosome RNA depletion, followed by cDNA synthesis and ligation of a universal tag. Ligated products were used for target enrichment by PCR amplification using the universal tag primer and a pool of primers targeting *ALK*, *ROS1,* and *RET* in a single tube (Z. Zheng et al, unpublished data). The resulting amplicons were directly sequenced using the Ion Torrent PGM system (Life Technologies).

## Results

### *ALK*, *ROS1,* and *RET* Fusion Assay Design

NanoString's technology is based on the dual hybridization of a capture and a molecularly bar-coded reporter probe complementary to a contiguous target sequence.[17–19] A 5′ capture probe consists of a target-specific, approximately 50-mer biotinylated probe, and a 3′ reporter probe consists of a target-specific, approximately 50-mer probe linked to six fluorescently labeled tags, the ordered combination of which dictate the unique assignment of a molecular bar code to each target-specific reporter. The direct hybridization of probe sets to RNA transcripts results in the formation of a tripartite complex of capture probe/RNA target/reporter probe. No cDNA synthesis or enzymatic steps are needed. On removal of excess probes, the hybridization complex is immobilized to a streptavidin-coated surface and aligned. The sequence-specific, fluorescently labeled reporter bar codes are digitally imaged using a charge-coupled device microscope and then are counted. The number of unique reporter bar codes specific to a target sequence is proportional to the number of transcripts present.

We previously demonstrated the performance of NanoString's technology to detect the presence or absence of

**Table 2** RT-PCR/Sanger Sequencing Primers

| Fusion variant | PCR forward primer | Sequence | RT-PCR reverse primer | Sequence |
|---|---|---|---|---|
| EML4-ALK; E2:A20 | EML4 exon 2 | 5′-AAGATCATGTGGCCTCAGTG-3′ | ALK exon 20R | 5′-CTTGCTCAGCTTGTACTCAGG-3′ |
| EML4-ALK; E6:A20 | EML4 exon 6 | 5′-CTGCAGACAAGCATAAAGATG-3′ | ALK exon 20R | 5′-CTTGCTCAGCTTGTACTCAGG-3′ |
| EML4-ALK; E13:A20 | EML4 exon 13 | 5′-GACTCGGTGGAGTCATGC-3′ | ALK exon 20R | 5′-CTTGCTCAGCTTGTACTCAGG-3′ |
| EML4-ALK; E18:A20 | EML4 exon 18 | 5′-AGGTGGTTTGTTCTGGATGC-3′ | ALK exon 20R | 5′-CTTGCTCAGCTTGTACTCAGG-3′ |
| EML4-ALK; E20:A20 | EML4 exon 20 | 5′-CAGATATGGAAGGTGCACTG-3′ | ALK exon 20R | 5′-CTTGCTCAGCTTGTACTCAGG-3′ |
| TFG-ALK; T5:A20 | TFG exon 5F | 5′-TCTACTCAGGTTATGGCAGCAA-3′ | ALK exon 20R | 5′-CTTGCTCAGCTTGTACTCAGG-3′ |
| KIF5B-ALK; K17:A20 | KIF5B exon 17F | 5′-CCTTCAAAATGTGGAACAAAA-3′ | ALK exon 20R | 5′-CTTGCTCAGCTTGTACTCAGG-3′ |
| KIF5B-ALK; K24:A20 | KIF5B exon 24F | 5′-TGAAAGCTTTGGAATCAGCA-3′ | ALK exon 20R | 5′-CTTGCTCAGCTTGTACTCAGG-3′ |
| SLC34A2-ROS1; S4:R32 | SLC34A2 exon 4F | 5′-CTTCTCGGATTTCTCTACTTTTTC-3′ | ROS1 exon 32R | 5′-TCTTCAGCTTTCTCCCACTG-3′ |
| SLC34A2-ROS1; S13del2046:R32 | SLC34A2 S13del2046F | 5′-GCAGGATGTCCCTGTCAAG-3′ | ROS1 exon 32R | 5′-TCTTCAGCTTTCTCCCACTG-3′ |
| CD74-ROS1; C6:R32 | CD74 exon 6F | 5′-CATTGGCTCCTGTTTGAAATG-3′ | ROS1 exon 32R | 5′-TCTTCAGCTTTCTCCCACTG-3′ |
| SDC4-ROS1; S2:R32 | SDC4 exon 2F | 5′-GAGCCCTACCAGACGATGAG-3′ | ROS1 exon 32R | 5′-TCTTCAGCTTTCTCCCACTG-3′ |
| EZR-ROS1; E10:R34 | EZR exon 10 | 5′-GGAGAGAGAGAAAGAGCAGATGA-3′ | ROS1 exon 34R | 5′-TGTAACAACCAGAAATATTCCAAC-3′ |
| KIF5B-RET; K15:R12 | KIF5B exon 15F | 5′-AACGAGCAGCTGAGATGATG-3′ | RET exon 12R-1 | 5′-TCCAAATTCGCCTTCTCCTA-3′ |
| KIF5B-RET; K16:R12 | KIF5B exon 16F | 5′-AGAAAGCACACAAACTGAGAGC-3′ | RET exon 12R-1 | 5′-TCCAAATTCGCCTTCTCCTA-3′ |
| KIF5B-RET; K22:R12 | KIF5B exon 22F | 5′-TGGAAGAGACAGTGGCAAAA-3′ | RET exon 12R-1 | 5′-TCCAAATTCGCCTTCTCCTA-3′ |
| KIF5B-RET; K23:R12 | KIF5B exon 23F | 5′-CGCTGCTCAGAAGCAAAAA-3′ | RET exon 12R-1 | 5′-TCCAAATTCGCCTTCTCCTA-3′ |
| CCDC6-RET; C1:R12 | CCDC6 exon 1F | 5′-GCTGAAGATAGAGCTGGAGACC-3′ | RET exon 12R-1 | 5′-TCCAAATTCGCCTTCTCCTA-3′ |
| CUX1-RET; C10:R12 | CUX1 exon 10F | 5′-TCTCATCGGCCAATCACTCC-3′ | RET exon 12R-2 | 5′-CCAAATTCGCCTTCTCCTAGAG-3′ |

ALK fusion transcript in archival NSCLC tissue samples.[14] The assay relied on a dual strategy of interrogation of ALK 3′ transcript overexpression and detection of specific EML4-ALK fusion transcript variants. The 3′ overexpression portion of the assay was designed to assess a discontinuous pattern of ALK expression in regions flanking the fusion transcript junction (Figure 1A). Endogenous ALK is normally not expressed in lung tissue; the expression of endogenous ALK is usually due to a fusion event whereby expression of the chimeric fusion transcript is driven by the promoter of its partner gene. An imbalance between 5′ and 3′ probe signals favoring higher reporter counts distal to known fusion junction sites is indicative of the presence of fusion transcript. In the same single-tube assay, fusion-specific probe sets were also included to detect the most frequently occurring EML4-ALK fusion variants. EML4-ALK fusions are characterized by variable truncations in EML4 universally fused to the ALK kinase domain usually beginning at ALK exon 20. EML4-specific capture probes and ALK-specific reporter probes were designed to hybridize to approximately 50 nucleotides of partnering EML4 exon and 50 nucleotides of the canonical ALK exon 20 junction (Table 1). Strong evidence for the presence of fusion transcript is indicated by a high 3′/5′ ratio complemented by high fusion-specific reporter counts (Figure 1B). In some cases, only a high 3′/5′ ratio is evident, still indicative of a fusion transcript likely carrying a novel variant or a variant whose sequence is not covered by our fusion probes. We successfully validated the assay in 66 archival NSCLC tissue samples and confirmed positive results by RT-PCR followed by sequencing.[14] Our calls were highly concordant with previous results obtained by FISH and IHC analyses.

We have since expanded the assay to detect ROS1 and RET fusions in addition to ALK. Similar to ALK 3′ overexpression, we designed probe sets across the entire ROS1 and RET transcripts flanking known fusion junctions. Eight expression probes were designed: four proximal (5′-1 to 5′-4) and four distal (3′-1 to 3′-4) to the most commonly known junction sites for ROS1 and RET fusions, as depicted in Figure 1, C and E, respectively (Table 1). Fusion-specific probe sets were also designed to detect 12 ROS1 and 8 RET fusion isoforms (Table 1). As with ALK, several fusion variants of ROS1 and RET shared the same downstream fusion junction, preventing assignment of a unique reporter bar code. For example, RET fusion variants consist of different combinations of KIF5B exons fused to RET

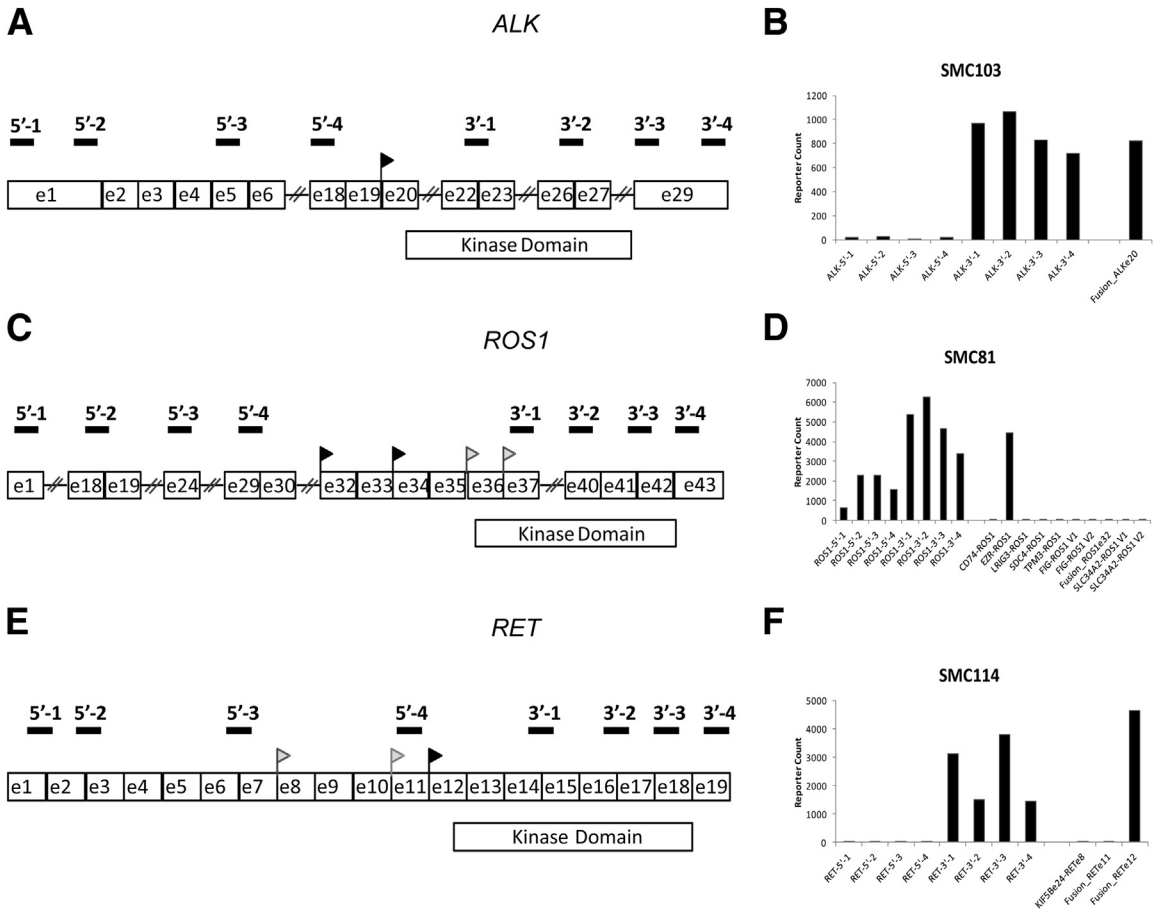


**Figure 1** ALK, ROS1, and RET fusion transcript assay design. Schematic representation of ALK (**A**), ROS1 (**C**), and RET (**E**) mRNAs and locations of gene expression probe sets relative to known fusion junction sites. Junction sites are depicted as filled flags (commonly occurring) and unfilled flags (less frequent). Representative expression profiles are shown for select patient samples positive for ALK (**B**), ROS1 (**D**), and RET (**F**) fusion transcripts.

exon 12. Because the same RET exon 12–specific reporter bar code is used, signal counts from that bar code ("Fusion_-RETe12") could signify the presence of any of the four variants bearing RET exon 12 sequence (Table 1). If necessary, further RT-PCR can be performed using different primer pairs to identify any one of the four possible variants. Representative expression profiles of select samples positive for ROS1 and RET are depicted in Figure 1, D and F, respectively.

## Detection of Fusion Transcripts from Minimal Tumor Cell Content and RNA Input

To determine the limit of detection and appropriate background threshold levels, we serially diluted RNA from cancer cell lines positive for *ALK* (NCI-H3122) or *ROS1* (HCC78) with increasing amounts of wild-type cell line (A549) RNA; no *RET* fusion–positive cell line was available at the time of testing. Fusion-positive cell lines were titrated down to varying percentages (100%, 50%, 25%, 12%, 6%, and 0%) relative to the fusion-negative cell line A549. A total of 250 ng of RNA was hybridized to the multiplexed assay comprising of a cocktail of 51 ALK, ROS1, and RET probes; 4 endogenous gene probes; and 6 positive and 8 negative spiked-in control probes. Figure 2 shows reporter counts normalized against spiked-in positive probes used to control for technical variability. When fusion-positive RNA samples were diluted with increasing amounts of negative control cell line RNA, fusion reporter counts showed a linear decrease in counts with an increasing percentage of wild-type cell line (Figure 2A). Background reporter counts in unspiked A549 were negligible, with reporter counts registering at 5 or below. In contrast, pure NCI-H3122 or HCC78 registered counts 2 and 3 log orders of magnitude, reaching background level at 6% ALK- or ROS1-positive RNA content. Figure 2B shows the geometric means of 5′ and 3′ expression probes for both serially diluted cell lines. A large separation between 5′ and 3′ probes was observed for each cell line titration, apparent even with only 6% of positive control cell line RNA. We interpret this to suggest that tumors containing at least 10% to 25% tumor cellularity can be detected using this assay.

In a previous ALK assay, we used 500 ng of RNA extracted from FFPE slides to maximize the chance of fusion detection. This high amount of RNA was arbitrarily chosen given the variability in tumor heterogeneity and the level of RNA degradation expected in clinical samples. We next explored the lowest possible amount of input RNA required to generate a fusion call. Three patient samples, SMC15 (ALK positive), SMC81 (ROS1 positive), and SMC85 (RET positive), previously ascertained by NanoString assay and confirmed by RT-PCR followed by sequencing were retested (Supplemental Figures S1A and S2B). By H&E staining, the samples exhibited 50% (SMC15), 90% (SMC81), and 95% (SMC85) tumor cell content. Starting from 500 ng of RNA, input amounts were decreased to 250, 100, 50, and 25 ng. From fusion reporter counts and separation of 3′ and 5′ expression levels, we approximated that at minimum, 50 to 100 ng of RNA is sufficient to predict the presence/absence of any of the three fusion transcripts (Figure 2, C and D). Note that of the three fusions, ALK is the least expressed. In a specimen containing 50% tumor cells and using 50 ng of input RNA, the ALK fusion reporter count was still above the background threshold level, and 3′ and 5′ expression levels were still widely separated (Figure 2, C and D).

## Assay Performance in Clinical Specimens

A total of 295 surgically resected lung adenocarcinoma samples were profiled with the multiplexed, single-tube assay to assess for inconsistent 3′ and 5′ expression levels and to directly detect the presence of fusion variants (Supplemental Table S1). To gauge the level of imbalance between 3′ and 5′ expression probes, we plotted the geometric mean of 5′ probes ($n = 4$) against the geometric mean

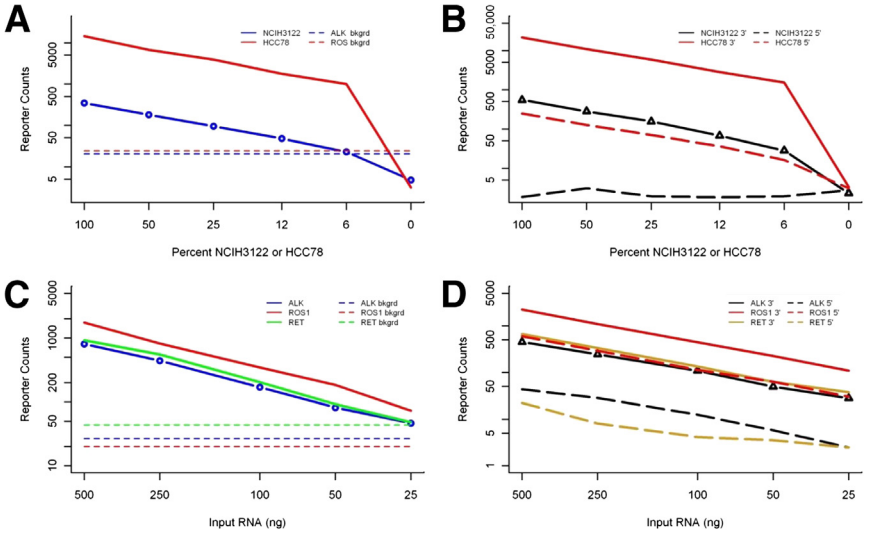


**Figure 2** Detection of fusion transcripts from minimal tumor cell content and RNA input. Reporter counts for cancer cell lines NCIH3122 (*ALK* positive) (**A**) and HCC78 (*ROS1* positive) (**B**) RNA serially diluted with increasing amounts of A549 RNA (*ALK* negative and *ROS1* negative). **A:** Fusion reporter counts as a function of varying RNA percentages of fusion-positive cell lines in a background (bkgrd) of wild-type cell line RNA. **B:** Geometric means of four 5′ and four 3′ expression probes as a function of varying percentages of fusion-positive lines. **C** and **D:** Expression profiles obtained from clinical samples previously confirmed positive for ALK, ROS1, and RET fusions (**C**) and corresponding reporter counts (**D**) with decreasing RNA input amounts.

of 3′ probes ($n = 4$) for each transcript (Figure 3, A, C, and E). More important, to visualize results obtained from the combined strategies in all the sample sets, we plotted the ratio of 3′/5′ expression to fusion reporter counts for each sample for ALK, ROS1, and RET (Figure 3, B, D, and F).

### *ALK*

Good cluster separation was obtained between IHC-positive (set 1, $n = 94$) and IHC-negative (set 2, $n = 85$) tumors, similar to what we previously observed.[14] ALK-negative samples exhibited low reporter counts (<100) in all expression probes, in contrast to ALK-positive samples, where reporter counts were higher in probes targeting 3′ than 5′ regions. We identified one sample (SMC152, the outlier at the top right corner in Figure 3A) that was ALK fusion positive by IHC analysis (score = 1) but ALK negative in our assay and confirmed as negative by FISH. This sample aberrantly expressed high levels of endogenous ALK in the absence of fusion, as signified by uniform 5′ and 3′ expression levels and low fusion reporter signal counts.

By plotting the 3′/5′ ratio to fusion reporter counts and applying thresholds for each, we were able to bin the samples into four quadrants (Figure 3). The threshold for ALK fusion probe count was determined to be approximately 60 in a previous publication,[14] and it could still be used for this larger data set. Figure 3B shows that a slightly lower threshold could work better, and as a result we decided to use two times the fusion background threshold $F_B$ as the threshold (approximately 50) for the ALK fusion probe. Distribution of the 3′/5′ ratio showed a cluster separation somewhere between twofold to fourfold; hence, we decided to use a cutoff value of threefold for the 3′/5′ ratio. We recognized that there were four samples with low fusion reporter counts whose 3′/5′ ratio bordered the cutoff threshold of 3. Given the ambiguity, it would be prudent to perform additional confirmation for this type of case.

We predicted 104 and 191 samples to be positive and negative for ALK fusion, respectively (Table 3). Note that set 1 was intentionally enriched for *ALK*-positive samples. Of the 104 *ALK*-positive samples, 88 met the positive criteria for both 3′ overexpression and high fusion counts (Figure 3B). Sixteen samples were also positive for 3′ overexpression but registered low fusion counts (Figure 3B). It is conceivable that these samples possess novel ALK variants or rare variants not covered by the fusion probes. For these samples, 5′ rapid amplification of cDNA ends or anchored multiplex PCR assay can be performed to identify possible novel ALK fusion partners. The present ALK fusion probe was designed to detect five EML4-ALK variants accounting

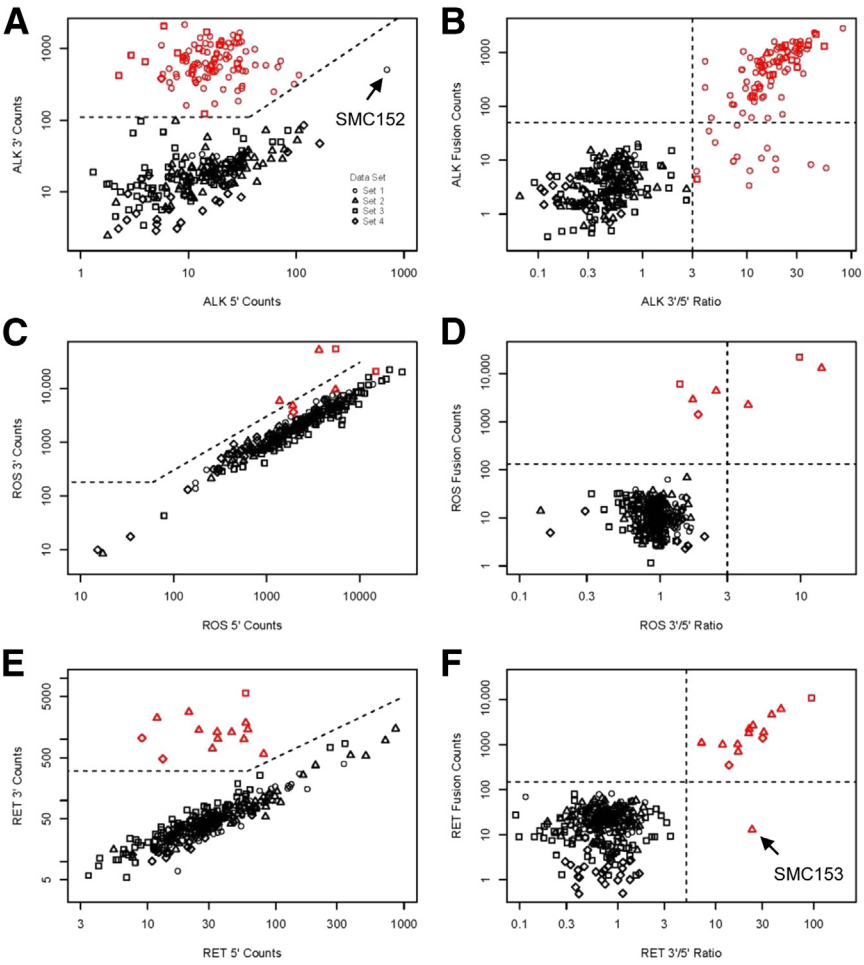


**Figure 3** Assay performance in clinical specimens. **A**, **C**, and **E:** Geometric means of 3′ and 5′ expression probes for ALK (**A**), ROS1 (**C**), and RET (**E**) transcripts. Background threshold levels are denoted by dashed lines. **B**, **D**, and **F:** Results were obtained from a dual strategy for ALK (**B**), ROS1 (**D**), and RET (**F**) profiling. Dashed lines denote thresholds applied for both fusion and 3′/5′ ratios. Fusion-positive and fusion-negative samples are depicted in red and black, respectively, and are noted by cohorts of origin (sets 1 to 4). SMC152 is ALK IHC 1+ but NanoString and FISH negative. SMC153 has an in-frame *CUX1-RET* fusion.

**Table 3** Incidence of *ALK*, *ROS1*, and *RET* Fusions

| Cohort | Clinical/molecular feature | Cases (No.) | | | |
|---|---|---|---|---|---|
| | | Total | ALK positive | ROS1 positive | RET positive |
| Set 1 | *ALK* IHC positive, *KRAS/EGFR* wild type | 94 | 91 | 0 | 0 |
| Set 2 | *ALK* IHC negative, *KRAS/EGFR* wild type | 85 | 1 | 4 | 11 |
| Set 3 | Never-smokers | 84 | 11 | 2 | 1 |
| Set 4 | Never-smokers with *ROS1* FISH data | 32 | 1 | 1 | 2 |
| Total | | 295 | 104 | 7 | 14 |

for 70% of major *EML4-ALK* fusion isoforms and two non–EML4-ALK variants (Table 1). As shown in Supplemental Figure S3, sequence determination of select *ALK*-positive samples confirmed the presence of EML4-ALK variants V1 (E13:A20), V2 (E20:A20), and a less frequently occurring variant V5′ (E18:A20).

Concordance of ALK IHC and FISH with the present assay is presented in Table 4. In cohort sets 1 and 2, in which 179 samples had IHC data and 52 samples had FISH data, we obtained concordance of 97.8% (175 of 179) for IHC and 100% for FISH. For IHC concordance analysis, agreement was determined between NanoString results and IHC data as categorized by the following staining scores: 0 = negative, 1 = weak, 2 = moderate, and 3 = strong. In 85 IHC-negative samples, we observed 1 discordant sample (SMC98) that was positive for ALK fusion in the assay. RT-PCR followed by sequence analysis of SMC98 confirmed expression of an ALK fusion transcript bearing EML4 exon 13 fused to ALK exon 20 (Supplemental Figure S3A). When IHC analysis was repeated, this sample was considered positive (IHC analysis score of 2). In five samples exhibiting weak IHC staining (score of 1), only three samples were concordant with NanoString results. The subsequent *ALK* FISH test showed that two NanoString negative/IHC (1+) tumors (SMC152 and SMC 195) were *ALK* FISH negative. SMC152 had a consistent level of expression throughout ALK 5′ and 3′ probe sets and low fusion reporter counts, indicating a high level of wild-type ALK expression. In samples with moderate ALK IHC staining, all 18 samples were concordant. In 71 samples with strong ALK IHC staining, we observed 1 discordant sample (SMC47), which was confirmed as negative by FISH as well. Comparing the results between NanoString and IHC analysis (Table 4), we calculated the assay's accuracy, sensitivity, and specificity to IHC analysis to be 97.8% (95% CI 94.4%–99.1%), 96.8% (91.0%–98.9%), and 98.8% (93.6%–99.8%), respectively. The Cohen kappa statistic on the agreement between IHC analysis (score 0 = negative, score 1 to 3 = positive) and our prediction is 0.944 (95% CI 0. 896–0.992). In these calculations, no FISH results were used. Among the 52 NSCLC tumors with ALK FISH data available, all the samples showed 100% concordance with NanoString results.

### *ROS1*

We observed a wide dynamic range in ROS1 expression level. Most samples expressed high levels of endogenous ROS1, with some samples exhibiting reporter counts well above 5000 (Figure 3C). In a small subgroup, endogenous ROS1 expression was low or absent despite good expression levels of endogenous control genes. Separation of 3′ and 5′ expression levels from the relatively few ROS1-positive samples was not as well defined as envisioned (Figure 3C) owing to high levels of endogenous ROS1 transcript obscuring the level of 3′ to 5′ overexpression. Nevertheless, positive samples can be identified clearly from fusion reporter results. In Figure 3D, we plotted the ratio of 3′/5′ to fusion counts and segregated the samples into four quadrants by applying thresholds for fusion reporter counts and the 3′/5′ ratio. In designating the fusion threshold, we selected five times $F_B$ as the fusion threshold (approximately 130) for *ROS1* because it is in the middle of the gap that separates the potential negative sample cluster and the positive sample cluster based on Figure 3D. For the 3′/5′ ratio threshold, based on cell line titration data (Figure 2A) that had serial dilutions of a positive sample where we found a threshold of 2 to 4 with good accuracy, we decided on a ratio of 3 to define the threshold. Both fusion probe and 3′/5′ ratio thresholds could be adjusted when more data are available. From these results, we predicted seven samples to be positive for ROS1 fusion. Note that four of the seven positive samples had high fusion counts but 3′/5′ ratios below the designated threshold of 3 (Figure 3D). The other three positive samples, however, exceeded the thresholds for both fusion and 3′/5′ ratio (Figure 3D). Seven positive samples from sets 2 to 4 were confirmed by RT-PCR followed by DNA sequencing. Four samples carried the EZR exon 10–ROS1 exon 34 fusion, two samples carried SLC34A2 exon 13del2046–ROS1 exon 32 fusion, and one sample carried CD74 exon 6–ROS1 exon 34 fusion (Table 5, Supplemental Figure S1). In cohort set 4 ($n$ = 32), which was analyzed by *ROS1* FISH (1 FISH-positive and 31 FISH-negative cases),[13] we observed 100% concordance between NanoString and FISH (Table 4). Three positive samples from set 2 (SMC81, SMC84, and SMC170) were also confirmed by FISH (Table 5).

### *RET*

Similar to ALK, the endogenous RET expression level was low such that a clear separation between 3′ and 5′ expression was apparent (Figure 3E). Although most samples exhibited reporter counts of 100 or less, a subgroup of samples expressed high RET levels without affecting the 3′/5′ separation. Plotting the 3′/5′ ratio with fusion reporter counts enabled us to designate appropriate thresholds (Figure 3F).

**Table 4** Concordance of ALK IHC and FISH Analyses as well as *ROS1* and *RET* FISH with the NanoString Assay

| | ALK IHC*† | | | | | *ALK* FISH‡ | | | *ROS1* FISH‡ | | | *RET* FISH‡ | | |
|---|---|---|---|---|---|---|---|---|---|---|---|---|---|---|
| NanoString | 0 | 1 | 2 | 3 | Total | FISH negative | FISH positive | Total | FISH negative | FISH positive | Total | FISH negative | FISH positive | Total |
| Positive | 1 | 3 | 18 | 70 | 92 | 0 | 46 | 46 | 0 | 4 | 4 | 0 | 11 | 11 |
| Negative | 84 | 2 | 0 | 1 | 87 | 6 | 0 | 6 | 42 | 0 | 42 | 4 | 0 | 4 |
| Total | 85 | 5 | 18 | 71 | 179 | 6 | 46 | 52 | 42 | 4 | 46 | 4 | 11 | 15 |

*ALK IHC staining is indicated by the following scores: 0, negative; 1, weak; 2, moderate; and 3, strong and number of ALK positive and ALK negative samples by NanoString assay.

†Accuracy of NanoString to IHC is 175/179 (97.8%) (SE = 1.1%, 95% CI =94.4%–99.1%); sensitivity is 91/94 (96.8%) (SE = 1.8%, 95% CI 91.0%–98.9%); specificity is 84/85 (98.8%) (SE = 1.2%, 95% CI 93.6%–99.8%); and Cohen kappa = 0.944 (SE = 0.025, 95% CI 0.896–0.992).

‡Accuracy of NanoString to *ALK* FISH is 52/52 (100%). Accuracy of NanoString to *ROS1* FISH is 46/46 (100%). Accuracy of NanoString to *RET* FISH is 15/15 (100%).

For fusion threshold determination, based on Figure 3F, we selected five times $F_B$ as the fusion threshold (approximately 150) for RET as it is in the middle of the gap that separates the potential negative sample cluster and the positive sample cluster. The 3′/5′ ratio was well separated for the RET gene (Figure 3F), and a threshold of five was chosen based on the gap between the cluster of samples that were likely negative and the cluster of samples that were potentially positive. These cutoff values could be adjusted as well when more data become available. We predicted 14 tumors to be positive for *RET* fusions. Thirteen of the 14 positive samples exceeded thresholds for both fusion and the 3′/5′ ratio (Figure 3F), and 1 tumor (SMC153) displayed a high 3′/5′ ratio but had a low fusion count, indicating the possible presence of a novel fusion. Using the anchored multiplex PCR assay followed by next-generation sequencing, we discovered that this adenocarcinoma possesses a novel *CUX1-RET* fusion (Figure 4A). This finding was further confirmed by FISH and RT-PCR, followed by Sanger sequencing (Figure 4, B–D). Exon 10 of the *CUX1* gene located on 7q22.1 was fused in-frame to exon 12 of RET located on 10q11.2. The coiled-coil domain of CUX1 and the kinase domain of RET are preserved in the CUX1-RET chimeric protein (Figure 4E). For the first time, we report discovery of a novel *CUX1-RET* fusion from a 49-year-old male smoker with a solid-type lung adenocarcinoma. The breakpoint sequence has been deposited in NCBI GenBank (*http://www.ncbi.nlm.nih.gov/genbank*, accession number KF421948, last accessed September 19, 2013). For the other 12 RET-positive samples, RT-PCR followed by DNA sequencing showed that 6 tumors carried fusions of KIF5B exon 15 to RET exon 12 and 6 carried fusions of CCDC6 exon 1 to RET exon 12 (Table 5, Supplemental Figure S2). We were unable to determine the exact fusion variant of one of the samples owing to poor RT-PCR results. Eleven RET-positive samples from set 2 were also confirmed by FISH (Table 5).

**Table 5** IHC, FISH, and RT-PCR/Sequencing Confirmation of Seven ROS1-Positive and 14 RET-Positive Cases

| ID | NanoString | *ALK* IHC | *ROS1* FISH | *RET* FISH | RT-PCR/Sanger sequencing |
|---|---|---|---|---|---|
| SMC77 | ROS1+ | Neg | ND | Neg | EZR Ex10–ROS1 Ex34 |
| SMC81 | ROS1+ | Neg | Pos | Neg | EZR Ex10–ROS1 Ex34 |
| SMC84 | ROS1+ | Neg | Pos | Neg | EZR Ex10–ROS1 Ex34 |
| SMC170 | ROS1+ | Neg | Pos | Neg | SLC34A2 Ex13del2046–ROS1 Ex32 |
| T17 | ROS1+ | ND | ND | ND | EZR Ex10–ROS1 Ex34 |
| T166 | ROS1+ | ND | ND | ND | SLC34A2 Ex13del2046–ROS1 Ex32 |
| YCC33 | ROS1+ | ND | Pos | ND | CD74 Ex6–ROS1 Ex34 |
| SMC55 | RET+ | Neg | Neg | Pos | CCDC6 Ex1–RET Ex12 |
| SMC56 | RET+ | Neg | Neg | Pos | KIF5B Ex15–RET Ex12 |
| SMC57 | RET+ | Neg | Neg | Pos | KIF5B Ex15–RET Ex12 |
| SMC67 | RET+ | Neg | Neg | Pos | CCDC6 Ex1–RET Ex12 |
| SMC69 | RET+ | Neg | Neg | Pos | CCDC6 Ex1–RET Ex12 |
| SMC74 | RET+ | Neg | Neg | Pos | KIF5B Ex15–RET Ex12 |
| SMC85 | RET+ | Neg | Neg | Pos | CCDC6 Ex1–RET Ex12 |
| SMC114 | RET+ | Neg | Neg | Pos | KIF5B Ex15–RET Ex12 |
| SMC118 | RET+ | Neg | Neg | Pos | KIF5B Ex15–RET Ex12 |
| SMC153 | RET+ | Neg | Neg | Pos | CUX1 Ex10–RET Ex12 |
| SMC179 | RET+ | Neg | Neg | Pos | CCDC6 Ex1–RET Ex12 |
| T232 | RET+ | ND | ND | ND | KIF5B Ex15–RET Ex12 |
| YCC3 | RET+ | ND | Neg | ND | ND |
| YCC14 | RET+ | ND | Neg | ND | CCDC6 Ex1–RET Ex12 |

ND, not determined; Neg, negative; Pos, positive.

The IHC, FISH, and RT-PCR/sequencing confirmation results of all the ROS1-positive ($n = 7$) and RET-positive ($n = 14$) samples identified in the study are summarized in Table 5. From the FISH analysis, ROS1-positive samples ($n = 4$) were not RET FISH positive and RET-positive samples ($n = 11$) were not ROS1 FISH positive.

### Mutual Exclusivity and Incidence of *ALK*, *ROS1*, and *RET* Fusions in NSCLC

The concurrent analysis of *ALK*, *ROS1*, and *RET* fusions in 295 NSCLCs showed that the fusions and *EGFR* and *KRAS* mutation status were mutually exclusive (Table 3, Supplemental Table S1). There were no *ROS1* and *RET* fusions found in cohort set 1 ($n = 94$), which was *ALK* positive, *EGFR* and *KRAS* wild type. Most *ROS1* ($n = 4$) and *RET* ($n = 11$) fusion–positive samples were found in cohort set 2 ($n = 85$), which was enriched for tumors negative for *ALK*, *EGFR*, and *KRAS* mutations. The frequency of *ROS1* and *RET* in this patient subgroup was much higher compared with unselected lung cancer patients, occurring at a frequency of 4.7% and 12.9%, respectively. In the third cohort of never-smokers with adenocarcinoma ($n = 84$, 77% females), the frequencies of *ALK*, *ROS1*, and *RET* fusions were 13%, 2.4%, and 1.2%, respectively.

## Discussion

Identification of the appropriate subset of patients likely to benefit from molecular targeted therapy is critical to the success of personalized medicine. The success of crizotinib in *ALK*-driven tumors and emerging clinical evidence of response in *ROS1*- and *RET*-rearranged tumors makes it imperative to develop practical screening methods to identify such patients for therapy. A single test capable of detecting any of the three rare *ALK*, *ROS1*, and *RET* fusions in lung cancer would be ideal as it would not only save time and money but also extend precious clinical specimens.

In this study, we developed and evaluated the performance of a transcript-based assay for the simultaneous detection of

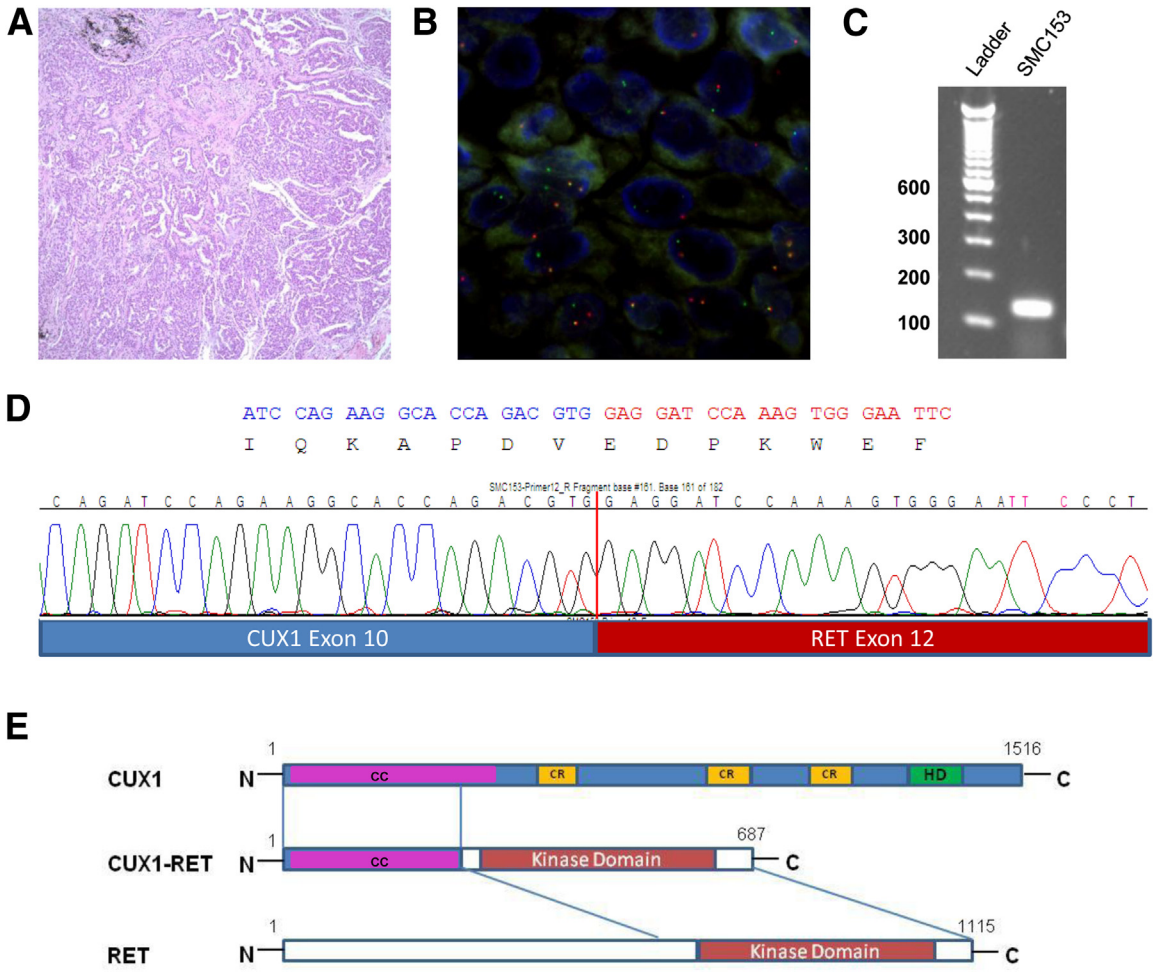


**Figure 4** *CUX1-RET* fusion. **A:** The tumor consists of adenocarcinoma, showing an acinar and papillary pattern. The tumor was positive for TTF-1 (data not shown). **B:** The break-apart RET FISH shows separate red and green signals in tumor cells. **C:** RT-PCR confirmation of CUX1-RET fusion. **D:** Sequence chromatogram of the CUX1-RET fusion junction sequence with protein sequence to demonstrate the in-frame reading frame. **E:** Schematic representation of the predicted CUX1-RET fusion protein. Original magnification (H&E), ×100 (**A**). CC, coiled-coil domain; CR, CUT DNA-binding domain; HD, homeobox domain.

*ALK, ROS1,* and *RET* fusions in lung cancer. The method is a single-tube, multiplexed assay designed to interrogate for the presence or absence of fusion transcripts using a single analyte. It incorporates two independent yet complementary strategies: the interrogation of imbalanced 3′/5′ expression levels and the direct detection of fusion transcript variants. The 3′ overexpression strategy does not require previous knowledge of fusion partners and relies mainly on the higher expression levels of probes distal to known fusion junctions of ALK, ROS1, and RET mRNA transcripts. This was the same strategy used by Suehara et al[20] to screen for tyrosine kinase fusion transcripts in lung adenocarcinomas. This approach is ideal for tumor types in which the endogenous transcript level is low such that there is a wide difference between fusion 3′ and endogenous 5′ expression levels, as in the case of ALK and RET. The direct fusion transcript detection and albeit limited ability to predict likely fusion variants from the fusion probes provide additional confidence in fusion calls. Notwithstanding, the assay can also pinpoint fusion-positive samples likely carrying novel fusion partners, as exemplified by the discovery of a novel *CUX1-RET* fusion.

For ROS1, elevated levels of endogenous ROS1 transcript somewhat obscured fusion 3′ overexpression. In NSCLC, microarray experiments showed elevated levels of ROS1 in 20% to 30% of tumors.[21–23] Tissue Northern blot analysis also showed that *ROS1* expression was highest in normal lung tissues.[24] Unless the 3′/5′ ratio is considerably high, assessment of imbalance in expression between 5′ and 3′ levels becomes difficult. In these instances, the direct detection of *ROS1* fusion transcripts via fusion probes augments the difficulty in assessment of ROS1 3′ overexpression.

NanoString's technology is notable for its high sensitivity, specificity, and wide dynamic range.[17–19,25] We have shown that we can readily detect fusion transcripts in cell line mixture containing at least 10% ALK or ROS1 fusion–positive transcript. This is consistent with a previous ALK assay where we were able to detect ALK fusion transcript in clinical samples with only 10% tumor content.[14] In our expanded assay consisting of 56 multiplexed probe sets, results were highly specific for each fusion, and background signal levels were considerably low. Although we have used 250 ng of fresh frozen or 500 ng of FFPE-derived clinical RNA in our assay evaluation, we have demonstrated that 50 to 100 ng of RNA from FFPE slide sections was sufficient for detection. This is especially relevant in specimens in which samples are limited, such as lung cancer. The wide dynamic range of the NanoString platform also allows for a single multiplex assay to detect any of the three fusions despite differences in levels of expression among the three. The ability to detect low abundant ALK and RET fusion transcripts in lung is another advantage of the system.

Current methods for the detection of ALK, ROS1, and RET fusions use FISH, IHC analysis, and/or RT-PCR, with each assay having its own advantages and disadvantages. Each fusion is tested separately, requiring multiple analytes, a concern where samples may be limited. Although FISH is the US Food and Drug Administration–approved diagnostic test for *ALK* rearrangement, screening a large number of patient samples by FISH for the three low-frequency fusions would be labor intensive and costly.[26] Certain fusion events, such as the ALK-PTPN3 fusion discovered from cancer genome sequencing,[27] may generate split-apart FISH signals but not respond to kinase inhibitors because the kinase domains are not preserved in such fusions. IHC analysis is a less expensive alternative, but high levels of endogenous protein may be challenging, especially for ROS1 analysis. In the case of ALK fusion detection, we have encountered instances of discordance between IHC and NanoString results. Because wild-type ALK transcript is not normally expressed in adult lung tissue, the aberrant expression of endogenous ALK rendered the samples ALK positive by IHC analysis. This was the case for tumor SMC152, where it was ALK IHC positive but negative in our assay as evidenced by uniform 3′ and 5′ *ALK* expression and low fusion reporter counts. The clinical benefit of *ALK* inhibition in these patients remains to be determined. Furthermore, diagnosis by both IHC and FISH is subjective in nature, with interobserver variability between laboratories being a potential source for false-positive/false-negative results. Because of this, we developed a quantitative scoring method using the NanoString assay by incorporating threshold settings for fusion determination. Although a benefit of RT-PCR allows for precise variant determination, the technology requires previous knowledge of fusion variants and use of multiple primer pairings, therefore missing all the yet-to-be-discovered fusion variants. Depending on the level of RNA degradation, some FFPE-derived RNA may not be amenable to downstream enzymatic reverse transcription and PCR reactions. One of the advantages of NanoString is its compatibility with RNA of variable quality (obtained from either fresh frozen or FFPE tissues) because it is based on hybridization of 50-mer oligo probes and does not require downstream enzymatic reactions.

We acknowledge that there are certain limitations to the present assay. Although the assay can provide presence/absence calls, it has certain limitations in predicting specific transcript variants. This is especially the case for variants sharing the same 3′ exon breakpoint that is recognized by the same reporter and, thus, the same bar code. Hence, as in the case of ALK, high signal counts arising from "Fusion_ALKe20" reporter indicate the presence of any one of the eight variants sharing the same ALK exon 20 target sequence. NanoString recently developed a new chemistry (Elements) where the placement of the reporter is now upstream of the fusion junction (ie, partnering transcript) as opposed to downstream (ie, canonical ALK exon 20), which theoretically will allow for variant discrimination. A high level of endogenous ROS1 also prevents reliable assessment of 3′ overexpression, although direct fusion detection can compensate for the limitation of 3′ overexpression strategy. Positive samples carrying potentially novel ROS1 fusions but exhibiting a low or near background 3′/5′ ratio can potentially be missed. Although the assay requires two to three FFPE slides of surgically resected tumors to generate

sufficient RNA for testing, analyzing needle biopsy samples may remain challenging. An amplification step could be considered to overcome the insufficiency of input materials.

In the present study, we identified *CUX1* as a novel fusion partner of *RET* in one male smoker with adenocarcinoma. *CUX1* belongs to the CUT homeobox family, which regulates gene expression, morphogenesis, and differentiation, and it may also play a role in cell-cycle progression as a homeobox transcription factor.[28] It consists of one coiled-coil, one homeobox, and three repetitive CUT DNA-binding domains (Figure 4E). Fusion of *CUX1* to *FGFR1* was previously reported in a patient with T-lymphoblastic leukemia/lymphoma with t(7;8)(q22;p11) translocation, in which CUX1 exon 11 was fused to FGFR1 exon 10.[29] *CUX1-FGFR1* fusion was able to transform the Ba/F3 cells to IL-3−independent growth, implicating its role in the pathogenesis of hematopoietic malignancies. In the present study, instead of exon 11, exon 10 of the CUX1 gene was fused to RET exon 12. Although the molecular mechanism underlying the role of *CUX1-RET* fusion in lung carcinogenesis is currently under investigation, the elevated expression of RET kinase domain caused by the fusion and the retained CUX1 N-terminal coiled-coil domain mediating dimerization suggest that fusion of *CUX1* to *RET* in NSCLC may result in constitutive activation of RET kinase and may trigger oncogenic cascade, as do the other *RET* fusions, such as *KIF5B-RET*.[30]

In summary, we developed a method for the simultaneous screening of *ALK*, *ROS1,* and *RET* fusions in NSCLC by direct, digital transcript profiling using NanoString's nCounter technology. The single-tube assay consolidates fusion tests for the three rare yet targetable fusions, offering a more practical screening modality. The assay is highly sensitive, quantitative, amenable to variable quality of RNA, easy to perform, semi-automated, and cost-effective. We believe that it shows promise for use as a prescreening tool in both research and clinical practice for the identification of a subset of patients with NSCLC most likely to benefit from specific targeted therapies.

## Acknowledgments

We thank John Iafrate, Long Le, and Zongli Zheng (Massachusetts General Hospital) and Jason Myers and Heather Peckham (ArcherDx Inc.) for anchored multiplex PCR assay reagents and technical assistance.

## Supplemental Data

Supplemental material for this article can be found at *http://dx.doi.org/10.1016/j.jmoldx.2013.11.007*.

## References

1. Kwak EL, Bang YJ, Camidge DR, Shaw AT, Solomon B, Maki RG, Ou SH, Dezube BJ, Janne PA, Costa DB, Varella-Garcia M, Kim WH, Lynch TJ, Fidias P, Stubbs H, Engelman JA, Sequist LV, Tan W, Gandhi L, Mino-Kenudson M, Wei GC, Shreeve SM, Ratain MJ, Settleman J, Christensen JG, Haber DA, Wilner K, Salgia R, Shapiro GI, Clark JW, Iafrate AJ: Anaplastic lymphoma kinase inhibition in non-small-cell lung cancer. N Engl J Med 2010, 363: 1693−1703
2. Chin LP, Soo RA, Soong R, Ou SH: Targeting ROS1 with anaplastic lymphoma kinase inhibitors: a promising therapeutic strategy for a newly defined molecular subset of non-small-cell lung cancer. J Thorac Oncol 2012, 7:1625−1630
3. Gu TL, Deng X, Huang F, Tucker M, Crosby K, Rimkunas V, Wang Y, Deng G, Zhu L, Tan Z, Hu Y, Wu C, Nardone J, MacNeill J, Ren J, Reeves C, Innocenti G, Norris B, Yuan J, Yu J, Haack H, Shen B, Peng C, Li H, Zhou X, Liu X, Rush J, Comb MJ: Survey of tyrosine kinase signaling reveals ROS kinase fusions in human cholangiocarcinoma. PLoS One 2011, 6:e15640
4. Li C, Fang R, Sun Y, Han X, Li F, Gao B, Iafrate AJ, Liu XY, Pao W, Chen H, Ji H: Spectrum of oncogenic driver mutations in lung adenocarcinomas from East Asian never smokers. PLoS One 2011, 6: e28204
5. Lipson D, Capelletti M, Yelensky R, Otto G, Parker A, Jarosz M, Curran JA, Balasubramanian S, Bloom T, Brennan KW, Donahue A, Downing SR, Frampton GM, Garcia L, Juhn F, Mitchell KC, White E, White J, Zwirko Z, Peretz T, Nechushtan H, Soussan-Gutman L, Kim J, Sasaki H, Kim HR, Park SI, Ercan D, Sheehan CE, Ross JS, Cronin MT, Janne PA, Stephens PJ: Identification of new ALK and RET gene fusions from colorectal and lung cancer biopsies. Nat Med 2012, 18:382−384
6. Rikova K, Guo A, Zeng Q, Possemato A, Yu J, Haack H, Nardone J, Lee K, Reeves C, Li Y, Hu Y, Tan Z, Stokes M, Sullivan L, Mitchell J, Wetzel R, Macneill J, Ren JM, Yuan J, Bakalarski CE, Villen J, Kornhauser JM, Smith B, Li D, Zhou X, Gygi SP, Gu TL, Polakiewicz RD, Rush J, Comb MJ: Global survey of phosphotyrosine signaling identifies oncogenic kinases in lung cancer. Cell 2007, 131: 1190−1203
7. Rimkunas VM, Crosby KE, Li D, Hu Y, Kelly ME, Gu TL, Mack JS, Silver MR, Zhou X, Haack H: Analysis of receptor tyrosine kinase ROS1-positive tumors in non-small cell lung cancer: identification of a FIG-ROS1 fusion. Clin Cancer Res 2012, 18:4449−4457
8. Takeuchi K, Soda M, Togashi Y, Suzuki R, Sakata S, Hatano S, Asaka R, Hamanaka W, Ninomiya H, Uehara H, Lim Choi Y, Satoh Y, Okumura S, Nakagawa K, Mano H, Ishikawa Y: RET, ROS1 and ALK fusions in lung cancer. Nat Med 2012, 18:378−381
9. Bergethon K, Shaw AT, Ou SH, Katayama R, Lovly CM, McDonald NT, Massion PP, Siwak-Tapp C, Gonzalez A, Fang R, Mark EJ, Batten JM, Chen H, Wilner KD, Kwak EL, Clark JW, Carbone DP, Ji H, Engelman JA, Mino-Kenudson M, Pao W, Iafrate AJ: ROS1 rearrangements define a unique molecular class of lung cancers. J Clin Oncol 2012, 30:863−870
10. Pao W, Hutchinson KE: Chipping away at the lung cancer genome. Nat Med 2012, 18:349−351
11. Seo JS, Ju YS, Lee WC, Shin JY, Lee JK, Bleazard T, Lee J, Jung YJ, Kim JO, Shin JY, Yu SB, Kim J, Lee ER, Kang CH, Park IK, Rhee H, Lee SH, Kim JI, Kang JH, Kim YT: The transcriptional landscape and mutational profile of lung adenocarcinoma. Genome Res 2012, 22: 2109−2119
12. Drilon A, Wang L, Hasanovic A, Suehara Y, Lipson D, Stephens P, Ross J, Miller V, Ginsberg M, Zakowski MF, Kris MG, Ladanyi M, Rizvi N: Response to cabozantinib in patients with RET fusion-positive lung adenocarcinomas. Cancer Discov 2013, 3:630−635
13. Kim HR, Lim SM, Kim HJ, Hwang SK, Park JK, Shin E, Bae MK, Ou SH, Wang J, Jewell SS, Kang DR, Soo RA, Haack H, Kim JH, Shim HS, Cho BC: The frequency and impact of ROS1 rearrangement on clinical outcomes in never smokers with lung adenocarcinoma. Ann Oncol 2013, 24:2364−2370
14. Lira ME, Kim TM, Huang D, Deng S, Koh Y, Jang B, Go H, Lee SH, Chung DH, Kim WH, Schoenmakers EF, Choi YL, Park K, Ahn JS, Sun JM, Ahn MJ, Kim DW, Mao M: Multiplexed gene expression and

fusion transcript analysis to detect ALK fusions in lung cancer. J Mol Diagn 2013, 15:51–61
15. Lee HJ, Seol HS, Kim JY, Chun SM, Suh YA, Park YS, Kim SW, Choi CM, Park SI, Kim DK, Kim YH, Jang SJ: ROS1 receptor tyrosine kinase, a druggable target, is frequently overexpressed in non-small cell lung carcinomas via genetic and epigenetic mechanisms. Ann Surg Oncol 2012, 20:200–208
16. Matsubara D, Kanai Y, Ishikawa S, Ohara S, Yoshimoto T, Sakatani T, Oguni S, Tamura T, Kataoka H, Endo S, Murakami Y, Aburatani H, Fukayama M, Niki T: Identification of CCDC6-RET fusion in the human lung adenocarcinoma cell line, LC-2/ad. J Thorac Oncol 2012, 7:1872–1876
17. Geiss GK, Bumgarner RE, Birditt B, Dahl T, Dowidar N, Dunaway DL, Fell HP, Ferree S, George RD, Grogan T, James JJ, Maysuria M, Mitton JD, Oliveri P, Osborn JL, Peng T, Ratcliffe AL, Webster PJ, Davidson EH, Hood L, Dimitrov K: Direct multiplexed measurement of gene expression with color-coded probe pairs. Nat Biotechnol 2008, 26:317–325
18. Malkov VA, Serikawa KA, Balantac N, Watters J, Geiss G, Mashadi-Hossein A, Fare T: Multiplexed measurements of gene signatures in different analytes using the NanoString nCounter assay system. BMC Res Notes 2009, 2:80
19. Reis PP, Waldron L, Goswami RS, Xu W, Xuan Y, Perez-Ordonez B, Gullane P, Irish J, Jurisica I, Kamel-Reid S: mRNA transcript quantification in archival samples using multiplexed, color-coded probes. BMC Biotechnol 2011, 11:46
20. Suehara Y, Arcila M, Wang L, Hasanovic A, Ang D, Ito T, Kimura Y, Drilon A, Guha U, Rusch V, Kris MG, Zakowski MF, Rizvi N, Khanin R, Ladanyi M: Identification of KIF5B-RET and GOPC-ROS1 fusions in lung adenocarcinomas through a comprehensive mRNA-based screen for tyrosine kinase fusions. Clin Cancer Res 2012, 18: 6599–6608
21. Bhattacharjee A, Richards WG, Staunton J, Li C, Monti S, Vasa P, Ladd C, Beheshti J, Bueno R, Gillette M, Loda M, Weber G, Mark EJ, Lander ES, Wong W, Johnson BE, Golub TR, Sugarbaker DJ, Meyerson M: Classification of human lung carcinomas by mRNA expression profiling reveals distinct adenocarcinoma subclasses. Proc Natl Acad Sci U S A 2001, 98:13790–13795
22. Garber ME, Troyanskaya OG, Schluens K, Petersen S, Thaesler Z, Pacyna-Gengelbach M, van de Rijn M, Rosen GD, Perou CM, Whyte RI, Altman RB, Brown PO, Botstein D, Petersen I: Diversity of gene expression in adenocarcinoma of the lung. Proc Natl Acad Sci U S A 2001, 98:13784–13789
23. Bild AH, Yao G, Chang JT, Wang Q, Potti A, Chasse D, Joshi MB, Harpole D, Lancaster JM, Berchuck A, Olson JA Jr., Marks JR, Dressman HK, West M, Nevins JR: Oncogenic pathway signatures in human cancers as a guide to targeted therapies. Nature 2006, 439:353–357
24. Acquaviva J, Wong R, Charest A: The multifaceted roles of the receptor tyrosine kinase ROS in development and cancer. Biochim Biophys Acta 2009, 1795:37–52
25. Kulkarni MM: Digital multiplexed gene expression analysis using the NanoString nCounter system. Curr Protoc Mol Biol 2011, Chapter 25: Unit25B 10
26. Atherly AJ, Camidge DR: The cost-effectiveness of screening lung cancer patients for targeted drug sensitivity markers. Br J Cancer 2012, 106:1100–1106
27. Jung Y, Kim P, Jung Y, Keum J, Kim SN, Choi YS, Do IG, Lee J, Choi SJ, Kim S, Lee JE, Kim J, Lee S, Kim J: Discovery of ALK-PTPN3 gene fusion from human non-small cell lung carcinoma cell line using next generation RNA sequencing. Genes Chromosomes Cancer 2012, 51:590–597
28. Hulea L, Nepveu A: CUX1 transcription factors: from biochemical activities and cell-based assays to mouse models and human diseases. Gene 2012, 497:18–26
29. Wasag B, Lierman E, Meeus P, Cools J, Vandenberghe P: The kinase inhibitor TKI258 is active against the novel CUX1-FGFR1 fusion detected in a patient with T-lymphoblastic leukemia/lymphoma and t(7;8)(q22;p11). Haematologica 2011, 96:922–926
30. Gainor JF, Shaw AT: Novel targets in non-small cell lung cancer: ROS1 and RET fusions. Oncologist 2013, 18:865–875